Specific Ion Effect of H$^+$ on Variably Charged Soil Colloid Aggregation

ZHANG Yekun, TIAN Rui*, TANG Jia, LI Hang**

Chongqing Key Laboratory of Soil Multi-Scale Interfacial Process, College of Resources and Environment, Southwest University, Chongqing, 400715, China

ABSTRACT

Specific ion effects have recently attracted the attention of soil scientists, and it has been found that ionic non-classic polarization plays an important role in the specific ion effect in soil. However, this explanation cannot be applied to H$^+$. The aim of this work was to characterize the specific ion effect of H$^+$ on variably charged soil (yellow earth) colloid aggregation. The total average aggregation (TAA) rates, critical coagulation concentrations (CCCs), activation energies, and the zeta potentials were used to characterize the specific ion effects. Results showed that strong specific ion effects of H$^+$, K$^+$, and Na$^+$ existed in variably charged soil colloid aggregation. The TAA rates, CCCs, and activation energies were sensitive to H$^+$, and a small amount addition of H$^+$ changed the TAA rates, CCCs, and activation energies markedly. The zeta potential results indicated specific ion effects of H$^+$, K$^+$, and Na$^+$ on soil aggregation were caused by specific ion effects of H$^+$, K$^+$, and Na$^+$ on the soil electric field strength. In addition, the origin of specific ion effect for H$^+$ was its chemical adsorption onto surfaces while those for alkali cations were non-classic polarization. This study indicated that H$^+$, which occurs naturally in variably charged soils, will dominate variably charged soil particle aggregation.

Key Words: Hofmeister effects, interaction energy,; zeta potential, dynamic light scattering

INTRODUCTION

Specific ion, or Hofmeister effects, first described in the 1880s as the different abilities of different ions to denature hen egg proteins, (Kunz *et al*., 2004) have recently attracted the attention of soil scientists (Sang *et al*., 2013; Liu *et al*., 2013, 2014; Tian *et al*., 2014, 2015a, b, c; Hu *et al*., 2015; Xu *et al*., 2015; Li *et al*., 2015; Du *et al*., 2016; Huang *et al*., 2016; Yu *et al*., 2016; Ballaha *et al*., 2016; Allen *et al*., 2017). Based on cation exchange and adsorption in clay suspensions, Liu *et al*. (2013, 2014) found strong specific ion effects on cation adsorption. They stated that the additional

interaction energy of K^+ adsorbed onto a permanently charged surface caused by the specific ion effect was approximately equal to the classic Coulomb interaction energy of K^+. In recent studies of cation adsorption kinetics, Du *et al.* (2016) found that specific ion effects of Cs^+, K^+, Na^+, and Li^+ adsorbed onto clay surfaces could give the cations effective/apparent charge numbers of +2.404, +1.942, +1.180, and +1.063, respectively.

Tian *et al.* (2014) found that specific cation effects strongly affect clay particle aggregation. The measured activation energies for montmorillonite aggregation in 25 mmol L^{-1} Li^+ solution were 1.2, 5.7, 28, and 126 times higher than in 25 mmol L^{-1} Na^+, K^+, Rb^+, and Cs^+ solutions, respectively. Tian *et al.* (2015c) also found strong specific anion effects on the aggregation of soils with variably charged surfaces, and the Hofmeister series for various anions was $H_2PO_4^- < Cl^- < NO_3^- < SO_4^{2-} < HPO_4^{2-} < PO_4^{3-}$. Specific ion effects on macroscopic phenomena such as soil aggregate stability (Hu *et al.*, 2015; Xu *et al.*, 2015; Huang *et al.*, 2016), soil water infiltration (Yu *et al.*, 2016), and soil erosion (Li *et al.*, 2015) have also been found.

Although the origin of specific ion effects on clay and soil systems was not clear, specific ion effects are closely related to the surface charges of soil particles and the electronic structures (or quantum states) of the cations and anions. Recently, non-classic cation or anion polarization has been suggested to create specific ion effects on clay and soil systems in general (Liu *et al.*, 2014; Hu *et al.*, 2015). Clay soil particles bear large amounts of surface charge, which can produce strong electric fields near the particle surfaces. The negative electric field near a clay particle surface could be approximate 10^8–10^9 V m^{-1} (Liu *et al.*, 2013; Hu *et al.*, 2015). The quantum state of an adsorbed cation could be strongly modified in such a strong electric field, causing the cation to be strongly non-classically polarized (Liu *et al.*, 2014; Hu *et al.*, 2015; Xu *et al.*, 2015). Ionic non-classic polarization could increase the adsorption energy for the surface cations (Du *et al.*, 2016) and therefore strongly screen the negative electric field around the soil/clay particles, further affecting the interaction energies between soil particles (Tian *et al*, 2014). This will affect the soil aggregate structure, soil pore stability (Hu *et al*, 2015; Xu *et al.*, 2015), soil erosion intensity (Li *et al.*, 2015), and soil water movement (Yu *et al.*, 2016).

However, the non-classic polarization scheme does not apply to H^+, which can also affect soil colloids, especially for soils with relatively large numbers of variable charges. H^+ is a special cation with no electrons around its nucleus. Polarization or non-classic polarization cannot occur for H^+. However, H^+ readily forms chemical bonds with soil/clay surface sites because its 1s electron orbit is empty and therefore has a strong affinity for the electrons of other atoms. It has been found that clay mineral particle aggregation is strongly affected by H^+ through Coulombic adsorption or coordinating-covalent-bond adsorption onto negatively charged surfaces (Tian *et al.*, 2015c; Kretzschmar *et al.*, 1998; Tombacz *et al.*, 2001; Gupta *et al.*, 2011; Wang *et al.*, 2017). Additionally, H^+ has a much smaller volume than other cations and can be treated as approximately a point-like charge. Liu *et al.* (2015) showed that volume effect of H^+ can strongly decrease the surface potentials of clay particles in an aqueous solution.

In this study, the specific ion effects of H^+, K^+, Na^+, $H^+ + Na^+$, and $H^+ + K^+$ on variably charged soil colloid aggregation were investigated. The total average aggregation (TAA) rates, critical coagulation concentrations (CCCs), and activation energies were measured and used to characterize the specific ion effects.

MATERIALS AND METHODS

2

Preparation of the colloid suspension

The colloid was extracted from yellow earth soil (Chongqing, China). The soil was air dried at room temperature, then gently crumbled and passed through a 1 mm mesh sieve. The bulk soil pH was 5.1 (soil/ultrapure water ratio of 1:5). The soil surface charge density was 0.197 C m^{-2} at pH 7, determine by the combined method (Li *et al*., 2011). The colloidal suspension was prepared (Tian *et al*., 2015c; Jia *et al*., 2013) using 50 g of the air-dried yellow earth soil that had been passed through a 0.25 mm sieve. The soil was added into a beaker, then 10 mL of 0.5 mol L^{-1} aqueous KOH and 500 mL of ultrapure water were added. The suspension was dispersed using an ultrasonic homogenizer probe (Scientz-IID, Ningbo, China) set to 20 kHz for 15 min, then diluted to 5000 mL with ultrapure water. The colloidal particles with effective hydrodynamic diameters < 200 nm were collected using the static sedimentation method, and the particles were concentrated by 0.5 mol L^{-1} HNO$_3$ solution. Finally, the concentrated colloids was washed repeatedly with ultrapure water until the effluent approached neutrality, then the suspension was adjusted to pH 8.0 by adding 0.1 mol L^{-1} KOH solution. This gave a K$^+$-saturated colloidal suspension. The colloidal suspension particle density, determined using the oven drying method, was 0.908 g L^{-1}. The colloidal suspension was diluted by a factor of 10 (giving a suspension at approximately pH 7) before dynamic light scattering experiments were performed. The effective hydrodynamic diameters of the colloidal particles were 50 − 500 nm, and a large proportion of the particles had hydrodynamic diameters around 192 nm (Fig. 1).

Fig. 1   The effective hydrodynamic diameter distribution of the primary colloidal particles

The clay mineral composition of the soil sample was determined using a freeze-dried aliquot of the colloid suspension. The sample was analyzed using an X-ray diffractometer (XRD-3, Beijing Purkinje General Instrument Co., Ltd., Beijing, China). The particles contained 6% kaolinite (d = 7.14 m), 8% gibbsite (d = 4.93 m), 41% illite (d = 4.45 m), 4% cristobalite (d = 4.16 m), 10% quartz (d = 3.34 m), 5% hematite (d = 2.68 m), 17% corundum (d = 2.55 m), and 9% goethite (d = 2.43 m) (Fig. 2). Low intensities were found when the particles were analyzed by X-ray diffractometry, possibly because the clay particles in the yellow soil sample were poorly crystalline (Fig. 2).

Fig. 2   X-ray diffraction curves of < 200 nm yellow soil particles

Dynamic Light Scattering (DLS) Measurements

DLS measurements were performed using a BI-200SM wide-angle laser light scattering instrument (Brookhaven Instruments Corp., New York) with a BI-9000AT autocorrelator operated using vertically polarized light at a wavelength of 532 nm and a scattering angle of 90 °. The laser device power was 15 mV. A 1 mL sample of a colloidal suspension was added, then selected concentrations of HCl, KCl, or NaCl solutions was added. The particle density of the mixed suspension was 0.09 g L^{-1}.

Single electrolyte tests were performed at the HCl concentrations (when mixed with the colloid suspension) of 0.1, 0.2, 0.3, 0.4, 0.5, 0.6, 0.7, 1, 2, 3, 4, and 5 mmol L^{-1}, the KCl concentrations of 5, 7, 8, 10, 15, 20, 25, 30, 35, and 40 mmol L^{-1}, and the NaCl concentrations of 5, 7, 10, 15, 20, 30, 40,

50, and 60 mmol L^{-1}. Mixed electrolyte tests using HCl + KCl or HCl + NaCl were first performed keeping the HCl concentration (when mixed with the colloid suspension) at 0.1 mmol L^{-1} and using the KCl concentrations of 0.2, 0.3, 0.4, 0.5, 0.7, 1, 2, 3, and 4 mmol L^{-1} and the NaCl concentrations of 0.2, 0.3, 0.4, 0.5, 0.7, 1, 2, 3, 4, and 5 mmol L^{-1}. The HCl concentration was then changed to 0.2 mmol L^{-1} and tests were performed using the KCl concentrations of 0.05, 0.1, 0.2, 0.4, 0.5, 1, 2, and 3 mmol L^{-1} and the NaCl concentrations of 0.1, 0.2, 0.5, 0.7, 1, 3, 4, and 5 mmol L^{-1}. The particle size distribution and aggregation kinetics were recorded every 30 s. The DLS measurements were performed at 298 ±0.5 K.

The repeatabilities for aggregation kinetics and zeta potential measurements were determined in the preliminary experiments. However, both measurements involved continuous and non-independent variables, so statistical analyses based on data for replicate analyses were unnecessary (such data can be found in other publications（Tian *et al.*，2014，2015c）). We therefore present the results of single experiments in the results section.

Determination of Aggregation Kinetics

Using the theory established by Jia *et al.* (2013), the TAA rate ($\tilde{v}_T(f_0)$, nm min^{-1}) for aggregation from the beginning of an experiment ($t = 0$) to time t_0 (> 0) can be expressed as

$$\tilde{v}_T(f_0) = \frac{1}{t_0} \int_0^{t_0} \frac{D(t) \quad D_0}{t} dt \qquad (1)$$

where f_0 (mmol L^{-1}) is the electrolyte concentration, and $D(t)$ (nm) and D_0 (nm) are the effective hydrodynamic diameters at time t (> 0) and at the beginning of the experiment ($t = 0$), respectively.

Two straight lines, representing for low and high electrolyte concentrations, could be fitted to the TAA rates. The lines corresponded to two different aggregation mechanisms. When there is a potential barrier between two adjacent particles, slow reaction-limited cluster aggregation (RLCA) occurs. As the potential barrier between the two particles disappears, fast diffusion-limited cluster aggregation (DLCA) occurs. (Gonzalez *et al.*, 1993; Klein *et al.*, 1989). Theoretically, the electrolyte concentration at the transition between RLCA and DLCA will be the CCC, which can be used to quantitatively characterize the colloid stability. The TAA rate would have been related to the activation energy $\Delta E(f_0)$ (J mol^{-1}), the minimum energy required for colloid aggregation, using the equations below (Li *et al.*, 2015).

$$\tilde{v}_T(f_0) = K \bullet f_0 \bullet e^{-\Delta E(f_0)/kT} \qquad (2)$$

$$K = \tilde{v}_T(CCC)/CCC \qquad (3)$$

In these equations, $\tilde{v}_T(CCC)$ is the TAA rate at $f_0 = CCC$, k is the Boltzmann constant, and T is the absolute temperature.

Zeta Potential Measurement

The zeta potentials of the colloidal particles were measured to investigate how the different

4

electrolytes affected colloid suspension coagulation. The zeta potential of the K^+-saturated colloid suspension was determined and used as the blank control. An electrolyte solution was then added to an aliquot of the K^+-saturated colloid suspension, and the suspension was shaken for 30 s. Tests were performed for each electrolyte or mixture at a series of concentrations. The zeta potential of each colloid suspension was measured every 15 min using a zeta potential instrument (ZetaPlus, Brookhaven Instruments, USA). The temperature was kept at 298 K. Each test was repeated three times.

RESULTS

Specific ion effects of H^+, K^+, and Na^+ on the aggregation kinetics of variably charged soil colloids

The average effective hydrodynamic diameters of the soil colloid particles in HCl, KCl, and NaCl at different concentrations are plotted against time (Fig. 3). Only aggregation curves at the same KCl and NaCl concentrations are shown to ensure that the difference between the results for K^+ and Na^+ tests are clear. Other experimental data was stated in the Supporting Information (Figure S1 and S2). It can be seen that H^+, K^+ and Na^+ had strong specific ion effects on soil particle aggregation (Fig. 3). At the same electrolyte concentration, the increases in the aggregate sizes increased in the order $H^+ \gg K^+ > Na^+$. The specific ion effect on the variably charged soil colloid aggregation kinetics was therefore stronger for H^+ than for K^+ or Na^+. For example, the average effective hydrodynamic diameters in the blank control, 5 mmol L^{-1} H^+, 5 mmol L^{-1} K^+, and 5 mmol L^{-1} Na^+ at 60 min were 192.6, 5236, 457, and 254 nm, respectively. The aggregates were 20.6 and 11.5 times bigger in the presence of H^+ than in the presence of Na^+ and K^+, respectively. Moreover, very little aggregation occurred in 5 mmol L^{-1} Na^+. The diameter versus time curves overlapped at HCl concentrations > 3 mmol L^{-1}, indicating that the maximum aggregation rate was reached. As for K^+ and Na^+, the maximum aggregation rates were reached at 15 mmol L^{-1} KCl and 30 mmol L^{-1} NaCl, respectively, or higher.

Fig. 3 The average effective hydrodynamic diameter of aggregates change with the aggregation time in HCl, KCl and NaCl solutions (mmol L^{-1})

The specific ion effects of H^+, K^+, and Na^+ on variably charged soil colloid aggregation kinetics were further investigated by measuring the soil colloid aggregation kinetics in mixed electrolyte solutions containing x mmol L^{-1} HCl + y mmol L^{-1} KCl or x mmol L^{-1} HCl + y mmol L^{-1} NaCl (Fig. 4). Figure 4 only show the aggregation curves at the same KCl and NaCl concentrations and other experimental data were stated in the Supporting Information (Figure S3 and S4). Adding only a small amount of H^+ to a K^+- or Na^+-saturated soil colloid suspension caused the particles size increasing dramatically, which indicated that the variably charged soil colloid aggregation rates were very sensitive to the presence of H^+. For example, hardly any aggregation occurred in the suspensions containing < 5 mmol L^{-1} KCl or NaCl (Fig. 3). However, the maximum aggregation rate at 2 mmol L^{-1} KCl or 3 mmol L^{-1} NaCl with only 0.1 mmol L^{-1} H^+ addition or at 1 mmol L^{-1} KCl or NaCl with 0.2 mmol L^{-1} H^+ (Fig. 4) addition can be reached.

Fig. 4 The average effective hydrodynamic diameter of aggregates change with aggregation time in mixture

electrolyte solutions of "x mmol L^{-1} HCl + y mmol L^{-1} KCl" and "x mmol L^{-1} HCl + y mmol L^{-1} NaCl" respectively (x = 0.1 and 0.2, y = 0.1, 0.2, 0.3, 0.4, 0.5, 1, 2, 3, 4 and 5)

Comparing the maximum aggregate sizes shown in Figs. 3 and 4 it can be seen that dramatically different sizes were found in the presence and absence of H$^+$. When no H$^+$ was added, the maximum aggregate size (~ 2000 nm shown in Fig. 3,) was found at high KCl and NaCl concentrations (15 and 30 mmol L^{-1}, respectively). However, adding 0.1 mmol L^{-1} H$^+$ caused the maximum aggregate size (~ 3100 nm shown in Fig. 4,) to be found at low KCl and NaCl concentrations (2 and 3 mmol L^{-1}, respectively).

Increasing H$^+$ concentration decreased the difference between the specific ion effects of K$^+$ and Na$^+$. For example, with no added H$^+$ (Fig. 3), the maximum aggregation rates were found at approximately 15 mmol L^{-1} K$^+$ and 30 mmol L^{-1} Na$^+$, i.e., a difference of 15 mmol L^{-1}, or, put another way, at a Na$^+$ concentration twice as high as the K$^+$ concentration. That is to say, the difference between the K$^+$ and Na$^+$ specific ion effects was relatively large at a H$^+$ concentration of ~ 0.0001 mmol L^{-1} (~ pH 7). However, at a H$^+$ concentration of 0.1 mmol L^{-1} (Fig. 4), the maximum aggregation rates were found at 2 mmol L^{-1} K$^+$ and 3 mmol L^{-1} Na$^+$, a difference of only 1 mmol L^{-1} or, put another way, at a Na$^+$ concentration 1.5 times higher than the K$^+$ concentration. Increasing the H$^+$ concentration to 0.2 mmol L^{-1} caused the difference in the specific ion effects of K$^+$ and Na$^+$ to disappear, the maximum aggregation rates being found at 1 mmol L^{-1} for both K$^+$ and Na$^+$. H$^+$ adsorption could decrease the surface charge density and therefore decrease the electrostatic field strength. Decreasing the electrostatic field strength would decrease the difference between the specific ion effects of K$^+$ and Na$^+$. The specific ion effects of K$^+$ and Na$^+$ therefore depended on the electrostatic field strength and could disappear at very weak electrostatic fields.

Specific ion effects of H$^+$, K$^+$ and Na$^+$ on the critical coagulation concentration

The TAA rates for solutions containing HCl, KCl, NaCl, HCl + KCl, and HCl + NaCl, which were estimated using Eq. (1), and the results showed that there were clear specific ion effects on the TAA rates (Figs. 5 and 6). The TAA rates in 5 mmol L^{-1} HCl, KCl, and NaCl were 192, 7.95, and 1.93 nm min^{-1}, respectively, i.e., the TAA rates in the presence of H$^+$ and K$^+$ were about 99 times and 4 times, respectively, larger than that of Na$^+$. The TAA rates in 10 mmol L^{-1} KCl and NaCl were 47.1 and 14.6 nm min^{-1}, respectively. The TAA rates increased in the order Na$^+$ < K$^+$ << H$^+$ (Fig. 5). As for the HCl + KCl and HCl + NaCl mixture (Fig. 6), given a total cation (H$^+$ + K$^+$ or H$^+$ + Na$^+$) concentration of 0.4 mmol L^{-1}, the TAA rates decreased in the order 0.1 mmol L^{-1} HCl + 0.3 mmol L^{-1} NaCl (20.2 nm min^{-1}) < 0.1 mmol L^{-1} HCl + 0.3 mmol L^{-1} KCl (26.8 nm min^{-1}) < 0.2 mmol L^{-1} HCl + 0.2 mmol L^{-1} NaCl (46.5 nm min^{-1}) < 0.2 mmol L^{-1} HCl + 0.2 mmol L^{-1} KCl (57.4 nm min^{-1}). The same sequence was found for the other total cation concentrations. The TAA rates for the HCl + KCl(or NaCl) mixture indicated that the TAA rates for the variably charged soil colloids were very sensitive to the presence of H$^+$. For example, the TAA rate was 0 nm min^{-1} at 0.3 mmol L^{-1} of KCl or NaCl when no H$^+$ was added (Fig. 5) whereas the TAA rates sharply increased to 20.2 and 26.7 nm min^{-1} for 0.3 mmol L^{-1} KCl and NaCl, respectively when only 0.1 mmol L^{-1} H$^+$ was added (Fig. 6).

Fig. 5 The TAA rates for the aggregation of soil particle as a function of electrolyte concentration f_0 in HCl, NaCl (pH ~ 7), KCl (pH ~ 7) solutions

Fig. 6 The TAA rates for the aggregation of colloidal particles as a function of KCl or NaCl concentration f_0 in mixture electrolyte solutions

The TAA rates changing with electrolyte concentrations can be fitted by two straight lines (Figs. 5 and 6), the concentration at the intersection was the CCC for the electrolyte system. The CCCs for the single electrolyte HCl, KCl, and NaCl systems (Fig. 5) were 0.88, 12.40, and 23.01 mmol L^{-1}, respectively (i.e., they increased in the order $H^+ << K^+ < Na^+$). This was consistent with the TAA rate pattern. The TAA rates at the CCCs decreased in the order H^+ (168 nm min^{-1}) $>> K^+$ (66.1 nm min^{-1}) $>> Na^+$ (59.8 nm min^{-1}). The CCCs for the mixed HCl + KCl and HCl + NaCl electrolyte systems (Fig. 6) were also very sensitive to the presence of H^+. At 0.1 mmol L^{-1} H^+, the CCCs decreased from 12.40 mmol L^{-1} KCl and 23.01 mmol L^{-1} NaCl to 1.20 mmol L^{-1} HCl + KCl and 1.29 mmol L^{-1} HCl + NaCl. At 0.2 mmol L^{-1} H^+, the CCCs for HCl + KCl and HCl + NaCl were even lower, 0.82 and 1.15 mmol L^{-1}, respectively.

Specific ion effects of H^+, K^+, and Na^+ on the aggregation activation energy

The activation energy $\Delta E(f_0)$ (in J mol^{-1}) is the minimum energy required for colloid aggregation to occur. The specific ion effects on variably charged soil particle aggregation were investigated further by estimating the $\Delta E(f_0)$ for the aggregation of soil particles in the presence of H^+, K^+, and Na^+. The $\Delta E(f_0)$ for soil particle aggregation in HCl, KCl, and NaCl solutions were estimated using Eq. (2) and (3), and strong specific ion effects on the activation energy were found (Fig. 7). At a constant electrolyte concentration, the activation energy increased in the order $H^+ << K^+ < Na^+$. In HCl solutions, the activation energy decreased sharply as the concentration increased at < 0.88 mmol L^{-1} and approached 0 J mol^{-1} at 0.88 mmol L^{-1}. However, the activation energy was very high at NaCl and KCl concentrations < 0.88 mmol L^{-1}, and aggregation did not occur at such low KCl and NaCl concentrations (Fig. 3).

Fig. 7 The Activation energy $\Delta E(f_0)$ for the aggregation of soil particles in HCl, KCl, NaCl solutions respectively

The $\Delta E(f_0)$ for soil particle aggregation in mixed HCl + KCl and HCl + NaCl solutions were estimated (Fig. 8). At a total cation ($H^+ + K^+$ or $H^+ + Na^+$) concentration of 0.4 mmol L^{-1}, the activation energy decreased in the order 0.1 mmol L^{-1} HCl + 0.3 mmol L^{-1} NaCl > 0.1 mmol L^{-1} HCl + 0.3 mmol L^{-1} KCl > 0.4 mmol L^{-1} HCl $\approx$ 0.2 mmol L^{-1} HCl + 0.2 mmol L^{-1} KCl > 0.2 mmol L^{-1} HCl + 0.2 mmol L^{-1} NaCl, indicating that the specific ion effects on the activation energy decreased in the order $H^+ >> K^+ > Na^+$. The activation energies for the HCl + KCl and HCl + NaCl mixtures further indicated that the activation energy for variably charged soil colloid aggregation was sensitive to H^+. For example, when no H^+ was added the activation energy approached to ∞ J mol^{-1} at high KCl and NaCl concentrations (3.42 and 5.11 mmol L^{-1}, respectively), but when 0.1 mmol L^{-1} H^+ was present the activation energy decreased sharply and was 0 J mol^{-1} at the low KCl and NaCl concentrations of 1.20 and 1.29 mmol L^{-1}, respectively. At a constant electrolyte concentration, the activation energies for the different electrolyte systems decreased in the order NaCl > KCl > 0.1 mmol L^{-1} HCl + NaCl > 0.1 mmol L^{-1} HCl + KCl > HCl $\approx$ 0.2 mmol L^{-1} HCl + KCl > 0.2 mmol L^{-1} HCl +

NaCl.

Fig. 8 The Activation energy ΔE (f_0) for the aggregation of soil particles in the various electrolyte solutions: HCl(—$\triangle$—), 0.2 mmol L^{-1}HCl+KCl(—$\bullet$—), 0.2 mmol L^{-1}HCl+NaCl(—$\blacklozenge$—), 0.1 mmol L^{-1}HCl+KCl(—$\triangledown$—), 0.1 mmol L^{-1}HCl+NaCl(—$\square$—)

The results described above indicated that (1) H^+, K^+, and Na^+ had strong specific ion effects on the TAA rates, CCCs, and activation energies for soil particle aggregation and that the specific ion effects decreased in the order $H^+ >> K^+ > Na^+$; and (2) the TAA rates, CCCs, and activation energies were sensitive to the presence of H^+ (i.e., they changed markedly when only a small amount of H^+ was added).

DISCUSSION

Interaction forces between particles determine the dynamics and stability of a colloidal suspension. Two interaction forces between particles, electrostatic repulsive and long-range van der Waals attractive forces, are considered in the Derjaguin–Landau–Verwey–Overbeek (DLVO) theory (Liang *et al*. 2007). It has been suggested that the non-DLVO surface hydration force also plays an important role in particle interactions in suspensions (Pashley *et al*., 1981, 1984; Ducker *et al*., 1992; Leng *et al*., 2012). However, Li *et al*. (2015) suggested that the surface hydration force does not influence the particle aggregation process in a suspension because the surface hydration force is often < 1.5 nm. Only the two DLVO forces should therefore be considered when studying colloid particle aggregation.

The Hamaker constant of a soil will theoretically not change under different electrolyte conditions in a suspension, so the van der Waals interaction force can be assumed to be the same for all the systems studied. However, the electrostatic repulsive force between soil particles strongly depends on the electrolyte conditions according to the DLVO theory (Pashley *et al*., 1981, 1984). The strength of the electrostatic repulsive force can be indirectly and qualitatively characterized by measuring the zeta potential. Under given electrolyte conditions in a suspension, a higher zeta potential indicates a stronger electrostatic force. The stronger the electrostatic force the higher the potential barrier or activation energy and therefore the lower the aggregation rate (Tian *et al*. 2014; Liu *et al*. 2015). Therefore, we measured the zeta potential of the particles under different electrolyte conditions of H^+, K^+, and Na^+ (Fig. 9). From the comparison between the zeta potentials and the TAA rates, CCCs as well as activation energies, we can see that the specific ion effects of H^+, K^+, and Na^+ on variably charged soil particle aggregation could generally be explained by the specific ion effects of H^+, K^+, and Na^+ on the electric field strengths around the soil particle surfaces.

Fig. 9 The zeta potentials change with electrolyte concentrations for different electrolyte solutions

Lower zeta potentials were found for the suspensions with added H^+ than that with K^+ or Na^+, the electrostatic repulsive energy between soil particles was therefore much lower in the presence of H^+ than in the presence of K^+ or Na^+. As a result, the soil aggregation rate and CCC were much higher and the aggregation energy much lower in the presence of H^+ than in the presence of K^+ or Na^+. However, the differences between the zeta potentials, aggregation rates, and activation energies for the

8

H$^+$ and K$^+$ or Na$^+$ systems increased with decreasing electrolyte concentration, especially at electrolyte concentrations < 1 mmol L^{-1} (Figs. 5, 7 and 9). Considering the volume effect of H$^+$, K$^+$ and Na$^+$ could be ignored at such low cationic concentration, (Liu *et al*. 2015), the large differences in the zeta potentials, TAA rates, CCCs, and activation energies were not caused by the H$^+$, K$^+$, and Na$^+$ cation sizes. In other words, the specific ion effects of H$^+$, K$^+$, and Na$^+$ on variably charged soil colloid particle aggregation could not be explained by the different sizes of the H$^+$, K$^+$, and Na$^+$ cations.

The zeta potentials, TAA rates, CCCs, and activation energies were very different in the presence of only a bit of H$^+$ than in the presence of K$^+$ or Na$^+$ (Figs. 5~9), implying that the physical mechanisms decreased the electric field strengths around the soil particles in the presence of H$^+$ and K$^+$/Na$^+$ were essentially different. The cations K$^+$ and Na$^+$ can be electrostatically adsorbed to the diffuse layer (DL) adjacent to a soil particle surface, so the electrostatic repulsive energy between soil particles in suspension was decreased by decreasing the DL thickness, leaving the negative charge density at the surface unchanged. However, H$^+$ can be adsorbed onto the surface of a variably charged soil particle surface through a coordinating covalent bond, which will sharply decrease the negative surface charge density. The zeta potential, TAA rate, CCC, and activation energy will therefore be changed markedly when a small amount of H$^+$ is added into the systems. However, the $\Delta E(f_0) \sim f_0$ curves for the suspensions in HCl, 0.1 mmol L^{-1} HCl + KCl, 0.1 mmol L^{-1} HCl + NaCl, 0.2 mmol L^{-1} HCl + KCl, and 0.2 mmol L^{-1} HCl + NaCl almost overlapped (Fig. 8), implying that all the particle surface sites formed coordinating covalent bonds with only 0.1 mmol L^{-1} H$^+$ addition, the small differences in the $\Delta E(f_0) \sim f_0$ curves were caused by the different degrees in compressing the DL thickness. If the sites available for chemical bond adsorption were not saturated at 0.1 mmol L^{-1} H$^+$, the activation energy will be markedly changed and thus the $\Delta E(f_0) \sim f_0$ curves could not overlap.

At ~ pH 7, the zeta potentials, TAA rates, CCCs, and activation energies for the suspensions were somewhat different for the suspensions containing K$^+$ and Na$^+$. Compared with Na$^+$ systems, the zeta potentials, CCCs, and activation energies in K$^+$ systems were lower while the aggregation rates were much higher. Differences between the results for K$^+$ and Na$^+$ systems were also found at low electrolyte concentrations, so different cation sizes and dispersion forces could not explain the specific ion effects of K$^+$ and Na$^+$ on soil colloid particle aggregation. Only the difference between non-classic polarization (Liu *et al*. 2014; Tian *et al*. 2014, 2015b) of K$^+$ and Na$^+$ in a strong electric field (the negative charge density is high at ~ pH 7) could reasonably explain the observed specific ion effects of K$^+$ and Na$^+$. K$^+$ is much more non-classically polarizable than Na$^+$, so the diffuse layer can be much more strongly compressed by K$^+$ than by Na$^+$. The electric field strength can therefore be decreased much more by K$^+$ than by Na$^+$.

CONCLUSIONS

Strong specific ion effects of H$^+$, K$^+$, and Na$^+$ on variably charged soil colloid aggregation were found. The soil aggregation rates decreased in the sequence of H$^+$ >> K$^+$ > Na$^+$, and the CCCs and activation energies increased in the order of H$^+$ << K$^+$ < Na$^+$. The TAA rates, CCCs, and activation energies were sensitive to the presence of H$^+$, and adding only a small amount of H$^+$ to a suspension markedly changed the TAA rate, CCC, and activation energy. The zeta potential results indicated that the specific ion effects of H$^+$, K$^+$, and Na$^+$ on soil aggregation were caused by the specific ion effects of H$^+$, K$^+$, and Na$^+$ on the surface electric field strength. Further analyses showed that the effect of H$^+$

on the electric field strength of a soil particle was mainly caused by coordinating covalent bond adsorption of H^+ to the variably charged soil particle surface because the electric field strength, CCC, and activation energy were much more strongly decreased by H^+ than by K^+ and Na^+. Nevertheless, the effects of K^+ and Na^+ on the electric field strength were mainly caused by compressing the diffuse layer. Our results also showed that the specific ion effects of K^+ and Na^+ on soil aggregation were caused by non-classic polarization of K^+ and Na^+. K^+ is much more non-classically polarizable than Na^+, so the diffuse layer will be compressed much more by K^+ than by Na^+ and the electric field strength will be decreased much more by K^+ than by Na^+. Variably charged soil (e.g., soil, such as an oxisol, with a relatively high number of variable charges) will have many H^+ cations at the particle surface, so our results indicate that H^+ will dominate variably charged soil particle aggregation.

ACKNOWLEDGEMENT(S)

REFERENCES

Allen N, Machesky M L, Wesolowski D J, Kabengi N. 2017. Calorimetric study of alkali and alkaline-earth cation adsorption and exchange at the quartz-solution interface. *J Colloid Interface Sci*. **504**: 538-548.

Ballaha J, Chameroisb M, Durand-Vidala S, Malikovaa N, Levitza P, Michota L J. 2016. Effect of chemical and geometrical parameters influencing the wettability of smectite clay films. *J Colloid Surf. A*. **511**: 255-263.

Du W, Li R, Liu X M, Tian R, Li H. 2016. Specific ion effects on ion exchange kinetics in charged clay. *Colloid Surf. A*. **509:** 427-432.

Ducker W A, Pashley R M. 1992. Forces between mica surfaces in the presence of rod-shaped divalent counterions. *Langmuir*. **8:**109-112.

Gonzalez A E. 1993. Universality of colloid aggregation in the reaction limit: the computer simulations. *Phys. Rev. Lett*. **71:** 2248-2251.

Gupta V, Hampton M A, Stokes J R, Nguyen A V, Miller J D. 2011. Particle interactions in kaolinite suspensions and corresponding aggregate structures. *J Colloid Interf Sci*. **359:** 95-103.

Hu F N, Li H, Liu X M, Li S, Ding W Q, Xu C Y, Li Y, Zhu L H. 2015. Quantitative Characterization of Non-Classic Polarization of Cations on Clay Aggregate Stability. *PLoS ONE* **10(4)**: 1-19.

Huang X R, Li H, Li S, Xiong H L, Jiang X J. 2016. Role of cationic polarization in humus-increased soil aggregate stability. *Eur. J. Soil Sci*. **67**: 341-350.

Jia M Y, Li H, Zhu H L, Tian R, Gao X D. 2013. An approach for the critical coagulation concentration estimation of polydisperse colloidal suspensions of soil and humus. *J. Soil Sediment*. **13:** 325-335.

Klein R, Meakin P. 1989. Universality in colloid aggregation. *Nature*. **339:** 360-362.

Kretzschmar R, Holthoff H, Sticher H. 1998. Influence of pH and humic acid on coagulation kinetics of kaolinite: A dynamic light scattering study. *J Colloid Interf. Sci* . **202:** 95-103.

Kunz W, Nostro P L, Ninham B W. 2004. The present state of affairs with Hofmeister effects. *Curr. Opin. Colloid Interface Sci.* **9**: 1-18.

Leng Y S. 2012. Hydration force between mica surfaces in aqueous KCl electrolyte solution. *Langmuir.* **28**: 5339-5349.

Li H, Hou J, Liu X M, Li R, Zhu H L, Wu L S. 2011. Combined Determination of Specific Surface Area and Surface Charge Properties of Charged Particles from a Single Experiment. *Soil Sci. Soc. Am. J.* **75**: 2128-2135.

Li Q Y, Tang Y, He X H, Li H. 2015. Approach to theoretical estimation of the activation energy of particle aggregation taking ionic nonclassic polarization into account. *AIP Adv.* **5**: 107218.

Li S, Li H, Hu F N, Huang X R, Xie D T, Ni J P. 2015. Effects of strong ionic polarization in the soil electric field on soil particle transport during rainfall. *Eur. J. Soil Sci.* **66**: 921-929.

Liang Y C, Hilal N, Langston P, Starov V. 2007. Interaction forces between colloidal particles in liquid: Theory and experiment. *Adv. Colloid Interface Sci.* **134-135:** 151-166.

Liu X M, Hu F N, Ding W Q, Tian R, Li R, Li H. 2015. A how-to approach for estimation of surface/Stern potentials considering ionic size and polarization. *Analyst* **140:** 7217-7224.

Liu X M, Li H, Du W, Tian R, Li R, Jiang X J. 2013. Hofmeister Effects on Cation Exchange Equilibrium: Quantification of Ion Exchange Selectivity. *J. Phys. Chem. C.* **117:** 6245-6251.

Liu X M, Li H, Li R, Xie D T, Ni J P, Wu L S. 2014. Strong non-classical induction forces in ion-surface interactions: General origin of Hofmeister effects. *Sci. Rep.* **4:** 5047.

Pashley R M. 1981. DLVO and hydration forces between mica surfaces in Li^+, Na^+, K^+, and Cs^+ electrolyte solutions: A correlation of double-layer and hydration forces with surface cation exchange properties. *J. Colloid Interface Sci.* **83:** 531-546.

Pashley R M, Israelachvili J N. 1984. DLVO and hydration forces between mica surfaces in Mg^{2+}, Ca^{2+}, Sr^{2+}, and Ba^{2+} chloride solutions. *J. Colloid Interface Sci.* **97:** 446-455.

Sang S L, Fenter P, Nagy K L, Sturchio N C. 2013. Changes in adsorption free energy and speciation during competitive adsorption between monovalent cations at the muscovite (001)-water interface. *J Geochimica Et Cosmochimica Acta.* **123**: 416-426.

Tian R, Yang G, Li H, Gao X D, Liu X M, Zhu H L, Tang Y. 2014. Activation energies of colloidal particle aggregation: towards a quantitative characterization of specific ion effects. *Phys. Chem. Chem. Phys.* **16:** 8828-8836.

Tian R, Yang G, Liu X M, Huang C Z, Gao X D, Li H. 2015a. Observation of the Unusual Aggregation Kinetics of Colloidal Minerals in Acidic Solutions. *J. Chem. Sci.* **127:** 1083-1089.

Tian R, Yang G, Tang Y, Liu X M, Li R, Zhu H L, Li H. 2015b. Origin of Hofmeister Effects for Complex Systems. *Plos One.* **10:** e0128602.

Tian R, Yang G, Zhu C, Liu X M, Li H. 2015c. Specific Anion Effects for Aggregation of Colloidal Minerals: A Joint Experimental and Theoretical Study. *J. Phys. Chem. C.* **119:** 4856-4864.

Tombacz E, Csanaky C, Illes E. 2001. Polydisperse fractal aggregate formation in clay mineral and iron oxide suspensions, pH and ionic strength dependence. *Colloid Polym Sci.* **279:**484-492.

Wang H, Zhao X, Han X, Tang Z, Liu S, Guo W, Deng C, Guo Q, Wang H, Wu F, Meng X, Giesy J P. 2017. Effects of monovalent and divalent metal cations on the aggregation and suspension of Fe_3O_4 magnetic nanoparticles in aqueous solution. *Sci. Total Environ.* **586:** 817-826.

Xu C Y, Li H, Hu F N, Li S, Liu X M, Li Y. 2015. Non-classical polarization of cations increases the stability of clay aggregates: specific ion effects on the stability of aggregates. *Eur. J. Soil Sci.* **66:** 615-623.

Yu Z H, Liu X M, Xu C Y, Xiong H L, Li H. 2016. Specific ion effects on soil water movement. *Soil Till. Res.* **161**: 63-70.
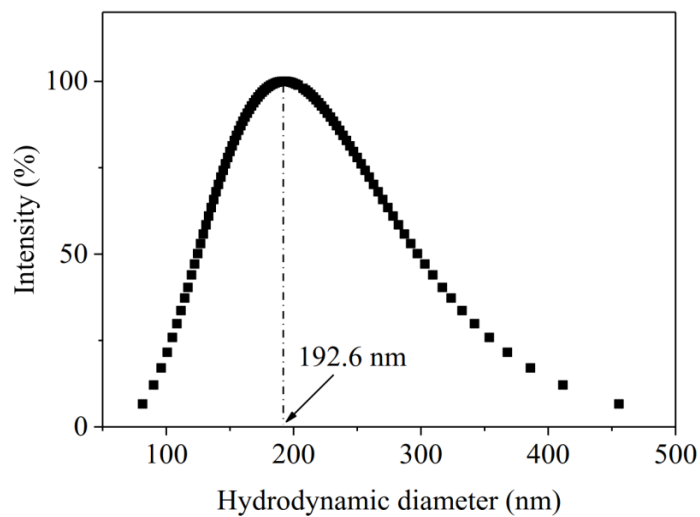
Figure 1: The effective hydrodynamic diameter distribution of the primary colloidal particles
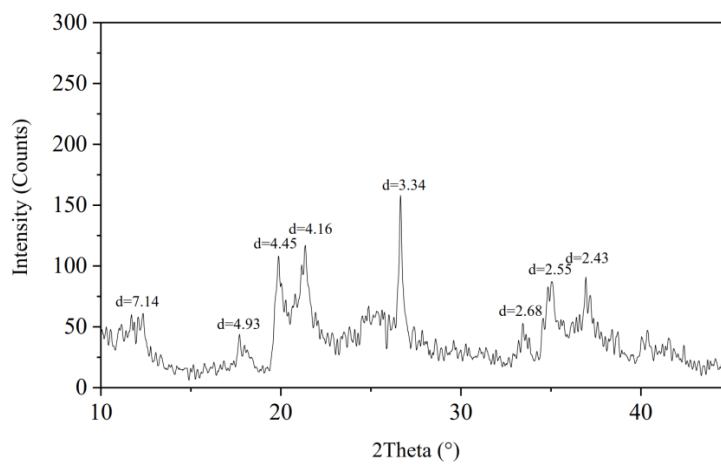
Figure 2: X-ray diffraction curves of < 200 nm yellow soil particles
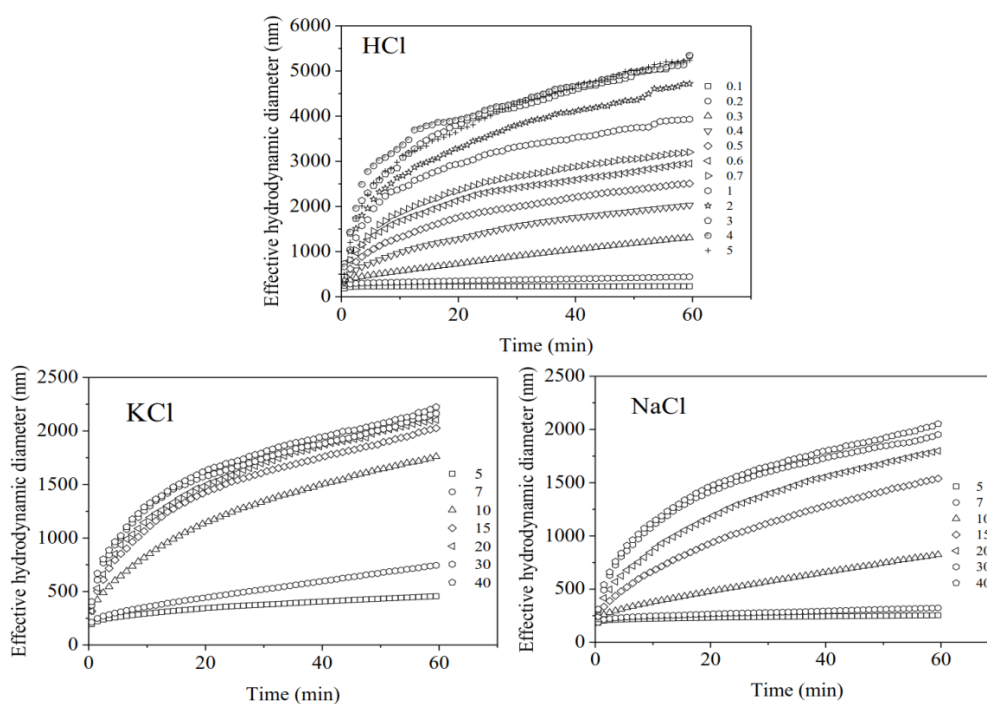
Figure 3: The average effective hydrodynamic diameter of aggregates change with the experiment time in HCl, KCl and NaCl solutions (mmol L^{-1})
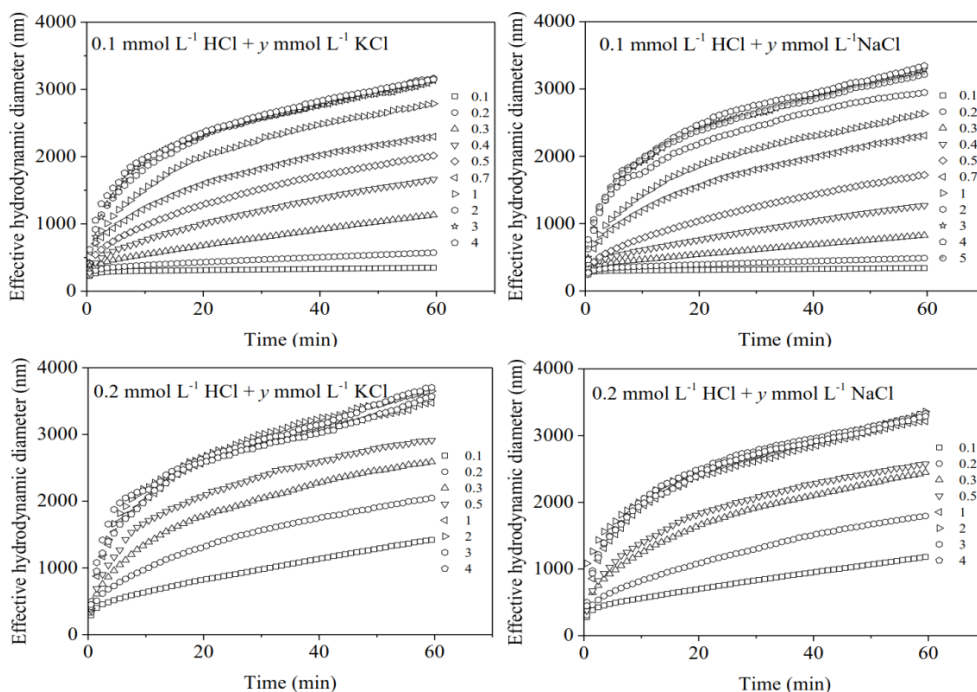
Figure 4: The average effective hydrodynamic diameter of aggregates change with the time in mixture electrolyte solutions of "x mmol L^{-1} HCl + y mmol L^{-1} KCl" and "x mmol L^{-1} HCl + y mmol L^{-1} NaCl" respectively ($x = 0.1$ and 0.2, $y = 0.1, 0.2, 0.3, 0.4, 0.5, 1, 2, 3, 4$ and 5)
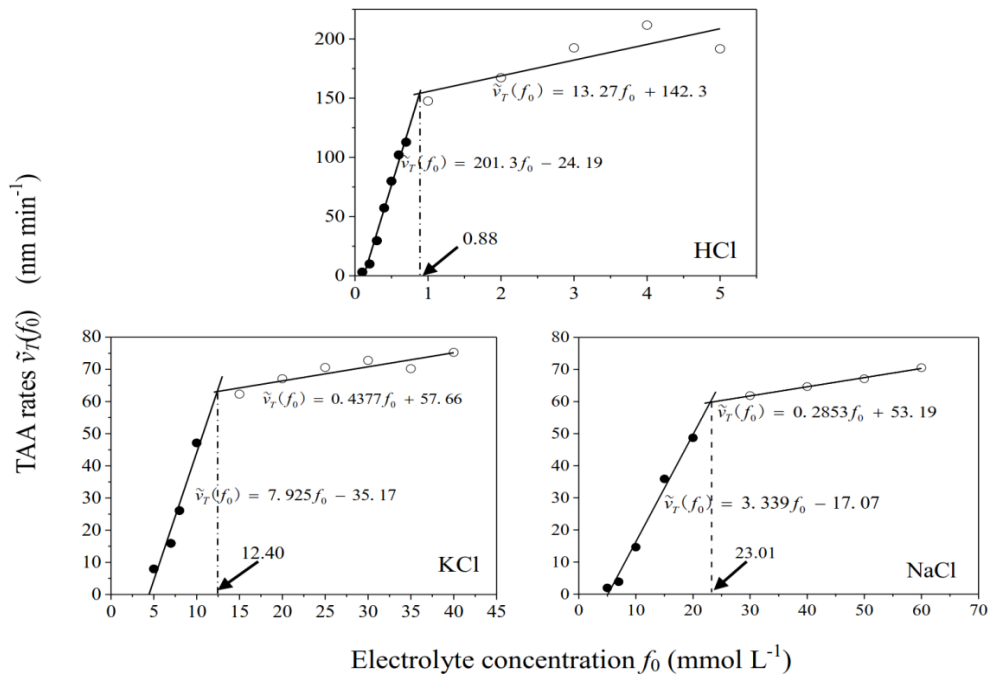
Figure 5: The TAA rates for the aggregation of soil particle as a function of electrolyte concentration f_0 in HCl, NaCl (pH ~ 7), KCl (pH ~ 7) solutions
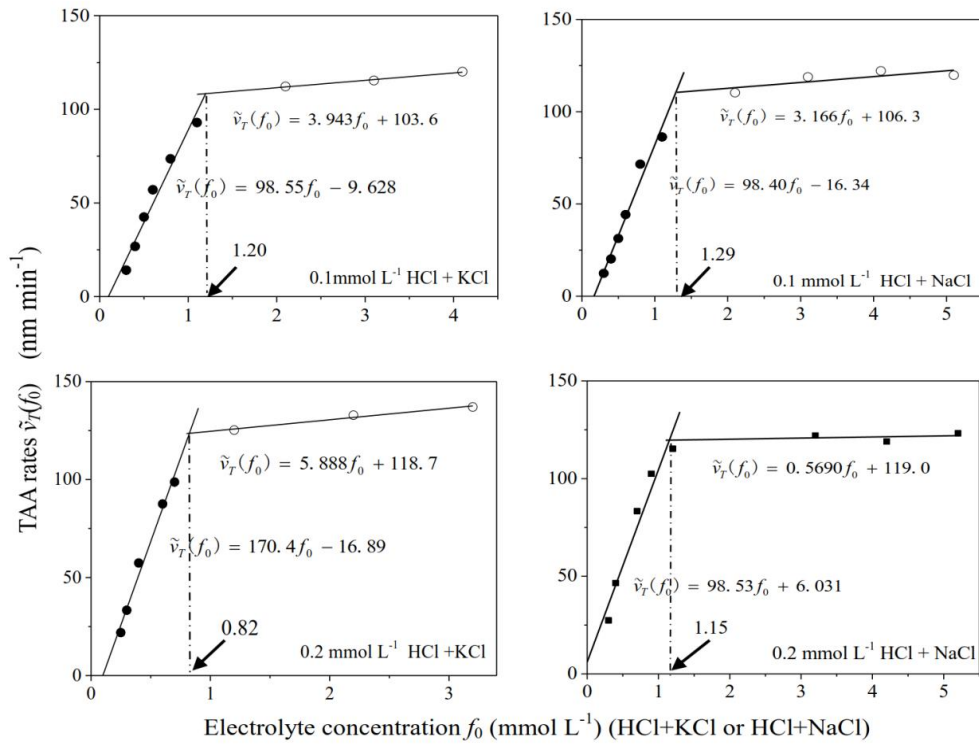
Figure 6: The TAA rates for the aggregation of colloidal particles as a function of KCl or NaCl concentration f_0 in mixture electrolyte solutions

14
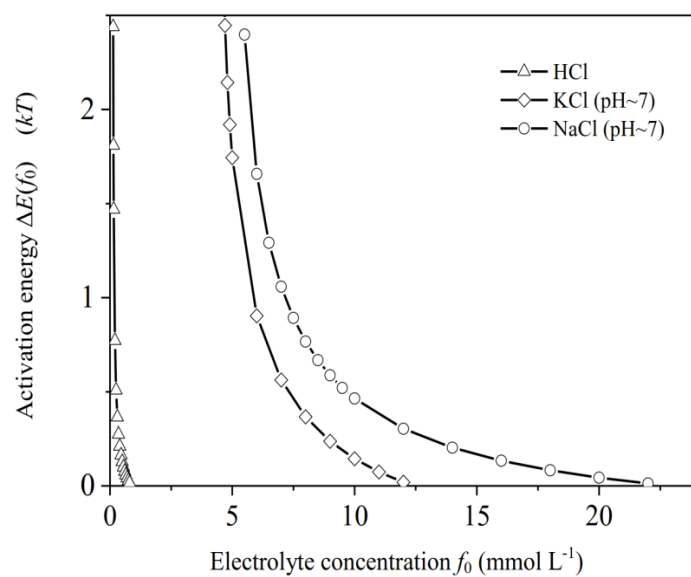
Figure 7: The Activation energy $\Delta E(f_0)$ for the aggregation of soil particles in HCl, KCl, NaCl solutions respectively
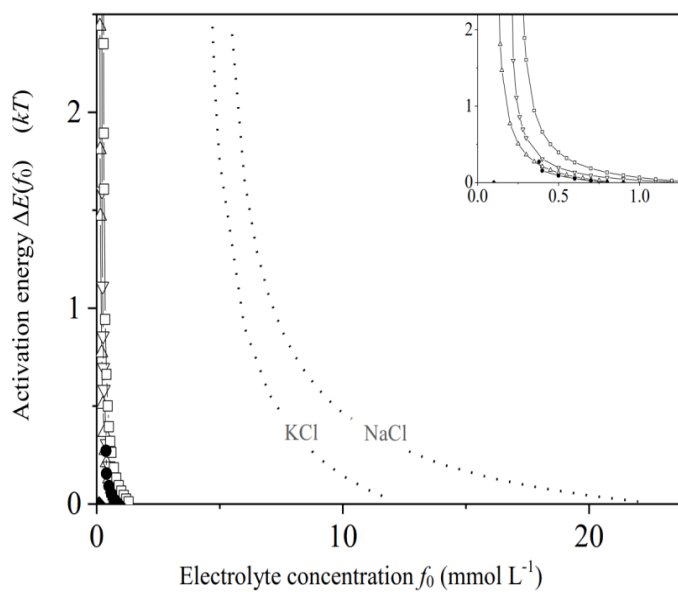
Figure 8: The Activation energy $\Delta E(f_0)$ for the aggregation of soil particles in the various electrolyte solutions: HCl(—△—), 0.2 mmol L^{-1}HCl+KCl(—●—), 0.2 mmol L^{-1}HCl+NaCl(—◆—), 0.1 mmol L^{-1}HCl+KCl(—▽—), 0.1 mmol L^{-1}HCl+NaCl(—□—)
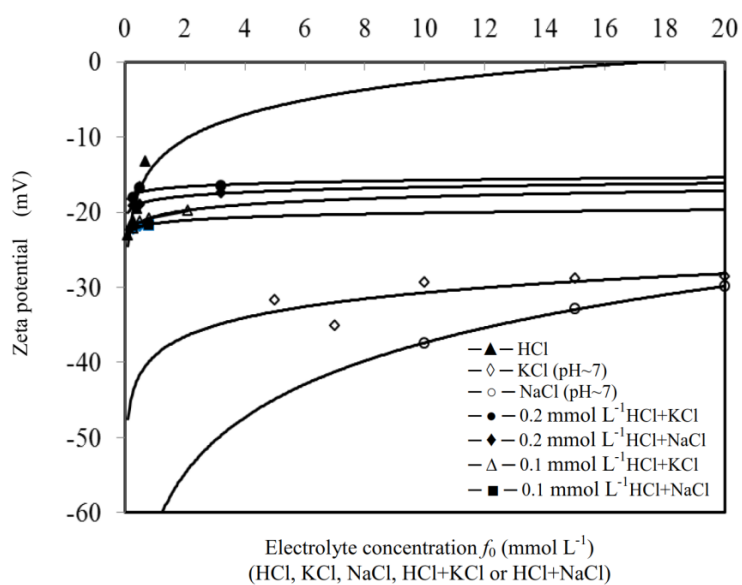
Figure 9: The zeta potentials change with electrolyte concentrations for different electrolyte solutions

Supplementary Information
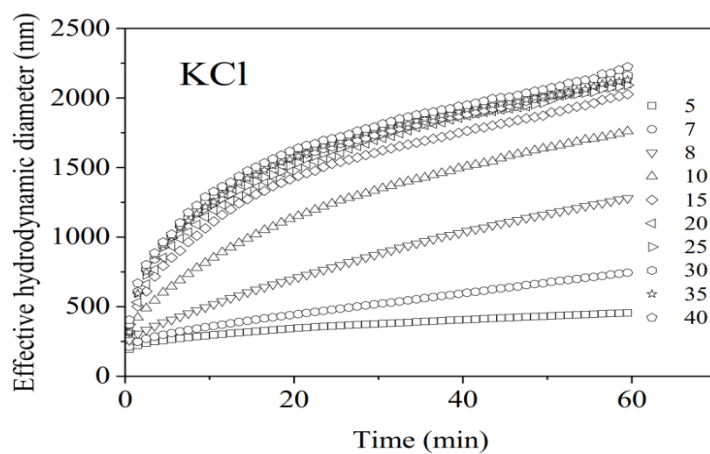
Figure S1: The average effective hydrodynamic diameter of the aggregates change with the experiment time in KCl solutions (mmol L-1)   **P.8**
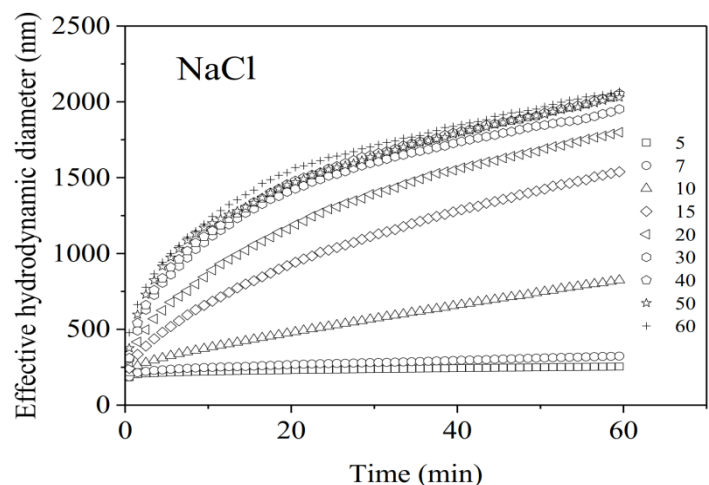
Figure S2: The average effective hydrodynamic diameter of the aggregates change with the experiment time in NaCl solutions (mmol L-1) **P.8**
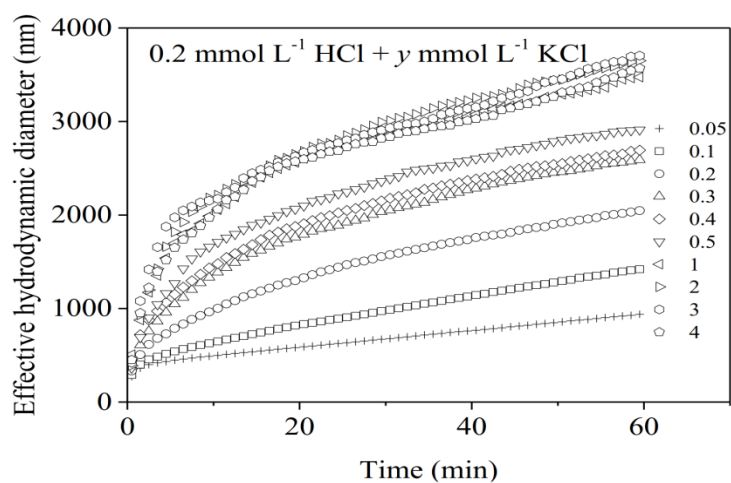
Figure S3: The average effective hydrodynamic diameter of aggregates change with aggregation time in mixture electrolyte solutions of "0.2 mmol L-1 HCl + y mmol L-1 KCl" (y = 0.05, 0.1, 0.2, 0.3, 0.4, 0.5, 1, 2, 3, 4) **P.9**
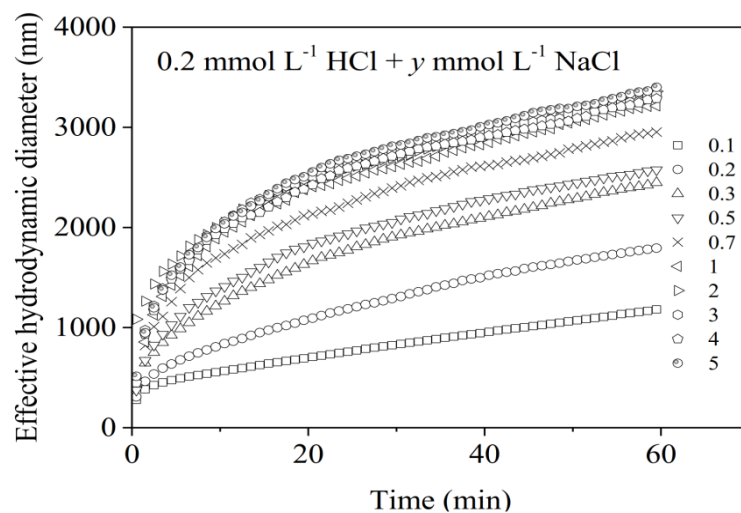
Figure S4: The average effective hydrodynamic diameter of aggregates change with aggregation time in mixture electrolyte solutions of "0.2 mmol L-1 HCl + *y* mmol L-1 NaCl" (*y* = 0.1, 0.2, 0.3, 0.5, 0.7, 1, 2, 3, 4 and 5) **P.9**